Talanta Open 13 (2026) 100644

Contents lists available at ScienceDirect

Talanta Open

journal homepage: www.sciencedirect.com/journal/talanta-open

A low-cost, battery-powered PCR thermocycler with enhanced thermal stability for on-site detection of harmful cyanobacteria

Ignasia Handipta Mahardika [a,1], Eunjin Huh [a,1], Yoseph Seo [b], Sarath Kin [a], Semin Chun [a], Sang Ho Lee [a], Sohyun Nam [a], Soo Ryeon Ryu [a], So Jung Kim [a,c], Shinwoo Kang [d], Wonseok Chung [d], Junhong Min [e], Taek Lee [b,*], Oh-Sun Kwon [a,*], Kwanwoo Shin [a,*]

[a] Department of Chemistry, Institute of Biological Interfaces, Lab311 Ltd. Co., Sogang University, Seoul 04107, Republic of Korea
[b] Department of Chemical Engineering, Kwangwoon University, Seoul 01897, Republic of Korea
[c] School of Biomedical Engineering, The University of British Columbia, Vancouver V6T 1Z3, Canada
[d] R&D Center for POCT, ctbio Ltd. Co., Dongtan 18471, Republic of Korea
[e] School of Integrative Engineering, Chung-Ang University, Seoul 06974, Republic of Korea

ARTICLE INFO

Keywords:
Portable PCR
Thermocycler
Point-of-care
Cyanobacteria
Harmful algal blooms

ABSTRACT

Harmful algal blooms (HAB), intensified by climate change and eutrophication, pose severe risks to freshwater ecosystems and public health, particularly in communities relying on surface water as drinking sources. Effective HAB surveillance requires rapid and reliable molecular detection tools that can be deployed directly in the field, yet most existing methods for detecting dominant freshwater cyanobacteria remain laboratory-bound, lacking the portability and affordability needed for on-site use. Here, we introduce the point-of-care testing polymerase chain reaction (POCT-PCR) device, a handheld, battery-powered thermocycler (1.0 kg, US$97) designed for on-site DNA amplification. The system integrates an aluminum heat sink, dual ceramic heaters, a Peltier-based cooling module, and a fast-response thermistor all governed by Arduino-based PID control. Using custom mini-PCR tubes with a 30 μL capacity, substantially smaller than the conventional 100 μL PCR tubes, to enhance thermal transfer and significantly minimize evaporation, the POCT-PCR achieves ramp rates of +1.10°C/s and –1.95°C/s, enabling fast and stable thermal cycling (30 cycles in 78 min). Validation assays confirmed reliable amplification of eleven cyanobacterial genes, including those associated with toxin-producing strains, with reproducibility comparable to benchtop systems. Field validation further confirmed the device's robustness and applicability under real environmental conditions. This low-cost platform enables rapid ecological surveillance and supports early-warning applications for harmful cyanobacterial blooms, expanding access to point-of-care molecular diagnostics for environmental and public health protection.

1. Introduction

The polymerase chain reaction (PCR) is a cornerstone technology in molecular biology, enabling the amplification of specific deoxyribonucleic acid (DNA) regions through repeated thermal cycling to generate millions of copies of a target sequence [1–6]. Since its development in the 1980s [1], PCR has become indispensable for clinical diagnostics, forensic science, food safety, and environmental monitoring of microbial communities [7–10]. In public health, PCR has established itself as the gold standard for pathogen detection, most notably during the COVID-19 pandemic, where its sensitivity and specificity provided reliable global surveillance capacity [7,11].

Over the past three decades, diverse PCR system formats have been introduced to improve speed, efficiency, and portability [12–22]. These include single-drop PCR [12], wafer-based ultrafast qPCR systems [12,13], polymer/glass-based chips [14–16], continuous-flow microfluidic devices [17–19], and capillary shuttling methods enabling so-called "Extreme PCR" [20]. Such innovations achieved remarkable heating and cooling ramp rates—up to +175°C/s and –125°C/s in wafer-based devices [12]—and cycle times as short as 0.42 s [20]. Despite these technical advances, however, the fundamental requirements for PCR remain stringent: precise thermal cycling, reproducible cycle times, and

* Corresponding authors.
E-mail addresses: tlee@kw.ac.kr (T. Lee), oskwon@sogang.ac.kr (O.-S. Kwon), kwshin@sogang.ac.kr (K. Shin).
[1] Co-first author: Both authors contributed equally to this work.

https://doi.org/10.1016/j.talo.2026.100644
Received 13 January 2026; Received in revised form 13 March 2026; Accepted 24 March 2026
Available online 24 March 2026
2666-8319/© 2026 The Authors. Published by Elsevier B.V. This is an open access article under the CC BY-NC license (http://creativecommons.org/licenses/by-nc/4.0/).

accurate temperature control are essential for fidelity [21–23]. Consequently, these systems often suffer from trade-offs. Ultrafast methods typically require specialized hardware and precise sample geometries [20], while continuous-flow or microfluidic devices involve complex fabrication and handling steps that limit accessibility and robustness in field-based applications [17–19]. Although non-contact heating methods, such as infrared, plasmonic heating, airflow, and Rayleigh-Bénard convection, have been explored, contact-based methods remain the most prevalent [24–27]. Consequently, miniaturization improves heat transfer by increasing the surface-to-volume ratio, which in turn reduces thermal capacity and shortens reaction times [24]. This enables the development of compact, rapid, and portable PCR platforms suitable for point-of-care testing (POCT) in resource-limited environmental monitoring contexts [13–16,21,22].

To meet practical needs outside the laboratory, several portable thermocyclers have been developed, often targeting POCT. For example, a US$100 battery-powered qPCR device based on a PDMS chip demonstrated field compatibility but required run times exceeding 80 minutes for 40 cycles [14]. As highlighted in Table 1, another system, costing approximately US$340, supported commercial PCR tubes with a 24-well capacity but still exhibited relatively slow thermal ramping rates (< +1.89°C/s, –1°C/s) [21]. A comparable $120 system utilizing the Arduino Uno R3 rather than the Mega 2560 [21] with a four-well capacity, was recently reported with ramping rates of +1.78°C/s and -1.52°C/s [22]. Other advancements include miniaturized chip- or microchannel-based PCR platforms powered by solar cells or rechargeable Li-ion batteries [28,29]. These devices illustrate the persistent challenge: balancing low cost, portability, and reliable amplification performance remains difficult, primarily due to limitations in heat transfer efficiency, sample evaporation, and the power demands of thermoelectric modules.

In the field, alternative detection strategies such as immunoassays, lateral flow strips, or spectroscopic sensors have been employed to provide rapid screening for pathogens or environmental markers. While convenient, these methods generally lack the specificity, reproducibility, and quantitative rigor of DNA-based approaches [9,10]. For decisive ecological and HAB-related interventions, PCR amplification remains the most reliable method. This underscores the critical need for portable thermocyclers capable of delivering accurate PCR amplification in resource-limited field environments.

One particularly urgent application is the monitoring of harmful cyanobacteria (often referred to as blue-green algae). Cyanobacterial blooms are intensifying worldwide due to eutrophication and rising global temperatures [30–34]. Many species produce potent toxins, including microcystins and cylindrospermopsin, which cause ecological damage, contaminate drinking water sources, and threaten human health. Outbreaks in freshwater reservoirs require rapid detection and immediate warning systems to mitigate risks for local communities relying on these resources [9,10,31]. While molecular assays for cyanobacteria have been reported [33,34], their application remains largely restricted to centralized laboratories. A portable PCR system that combines affordability, robustness, and on-site functionality would therefore be transformative for ecological surveillance and early detection of harmful algal blooms.

Here, we present the POCT-PCR system, a handheld, low-cost, and battery-powered thermocycler designed for rapid field detection of cyanobacterial DNA. The device integrates efficient heat transfer, precise Arduino-based proportional–integral–derivative (PID) temperature control, and custom mini-PCR tubes that minimize evaporation and enhance sample handling as shown in Fig. 1. We demonstrate successful amplification of eleven cyanobacterial genes, validating POCT-PCR as a reliable and practical platform for field-based genetic analysis. This approach highlights the feasibility of expanding DNA-based diagnostics beyond laboratory settings, enabling ecological monitoring and early-warning strategies for harmful cyanobacterial blooms.

2. Materials and methods

2.1. POCT-PCR thermocycler

The POCT-PCR device was constructed around an aluminum heat sink (Al6061-T6, 20 × 20 × 5 mm), into which three cylindrical sample tunnels (3.2 mm diameter, 18 mm depth) were drilled (Fig. 1). Dual ceramic heaters (20 × 20 × 2 mm, A54, Scipia, Korea) were positioned above and below the heat sink to ensure rapid thermal exchange. Temperature was monitored using a 10 kΩ bead-type NTC thermistor (NTC-103F397, Samkyung, Korea), calibrated against a temperature controller (CT425B, Minco, MN, USA). For active cooling, a thermoelectric Peltier module (TEC-12704, SMG, Korea) with aluminum finned heat sink was integrated, aided by two fans: a high-speed brushless fan (11,000 rpm) mounted above the fins and a low-speed fan (3,000 rpm) at the front chamber outlet to expel hot air.

Thermal control was implemented through an Arduino Nano R3 microcontroller (Arduino AG, Italy), which delivered pulse-width modulation (PWM) to n-type metal–oxide–semiconductor field-effect transistors (MOSFETs, IRLZ44N, Infineon Technologies, Germany) regulating the heaters, Peltier module, and fans. The electronic layout was designed in Fritzing (Interaction Design Lab, Potsdam, Germany), and the system was powered by a dual-battery configuration: a 12.8 V $LiFePO_4$ pack (3300 mAh, Powercraft, Korea) for the thermocycler and a 7.4 V Li-ion pack (2200 mAh, CADU Co., China) for control electronics. The assembled device weighed 1.0 kg and was housed in a laser-cut wooden case. All materials and components for POCT-PCR thermocycler were listed in Tables S1 and S2 of Supporting Information (S1 File in Appendix B), and the operating procedure is provided in a movie clip (S2 File). Circuit diagrams, PCB files, and firmware are provided in the Supporting Information (S3 – S6 Files).

2.2. PCR sample tube and plug cap

Custom PCR tubes were fabricated from semi-transparent silicone tubing (inner diameter 2.0 mm, outer diameter 3.0 mm, length 15 mm;

Table 1
The comparison of portable PCR thermocyclers.

Reference	Kadja *et al.* [21]	Luo *et al.* [22]	Yang *et al.* [28]	Kulkarni *et al.* [29]	This study
PCR container (number)	Commercial PCR tube (24)	Commercial PCR tube (4)	Commercial PCR tube (7)	Continuous channel (1)	Mini tube (3)
Cycle number	40	30	Isothermal 37°C	30	30
Total PCR time (minutes)	140	72	30	19	78
Heating/Cooling ramp rates (°C/s)	<+1.89/-1.0	+1.78/-1.52	+2.2/None	+0.58/None	+1.10/-1.95
Detection method	Fluorescence	Electrophoresis	Fluorescence	Photometric	Electrophoresis
Dimension/Weight (L x W x H, mm)/(kg)	210 × 160 × 200 /Not provided	210 × 140 × 105 /0.67	Not provided	150 × 100 × 50 /Not provided	220 × 90 × 80 /1.0
Microcontroller	Arduino Mega 2560	Arduino Uno R3	Not provided	Arduino Uno R3	Arduino Nano R3
Power	64 V, 2 A	15.5 V, 8 A	Solar cell UV flashlight	12 V	12.8 V, 2 A/ 7.4 V, 1 A
Cost (US$)	340	120	10	47	97

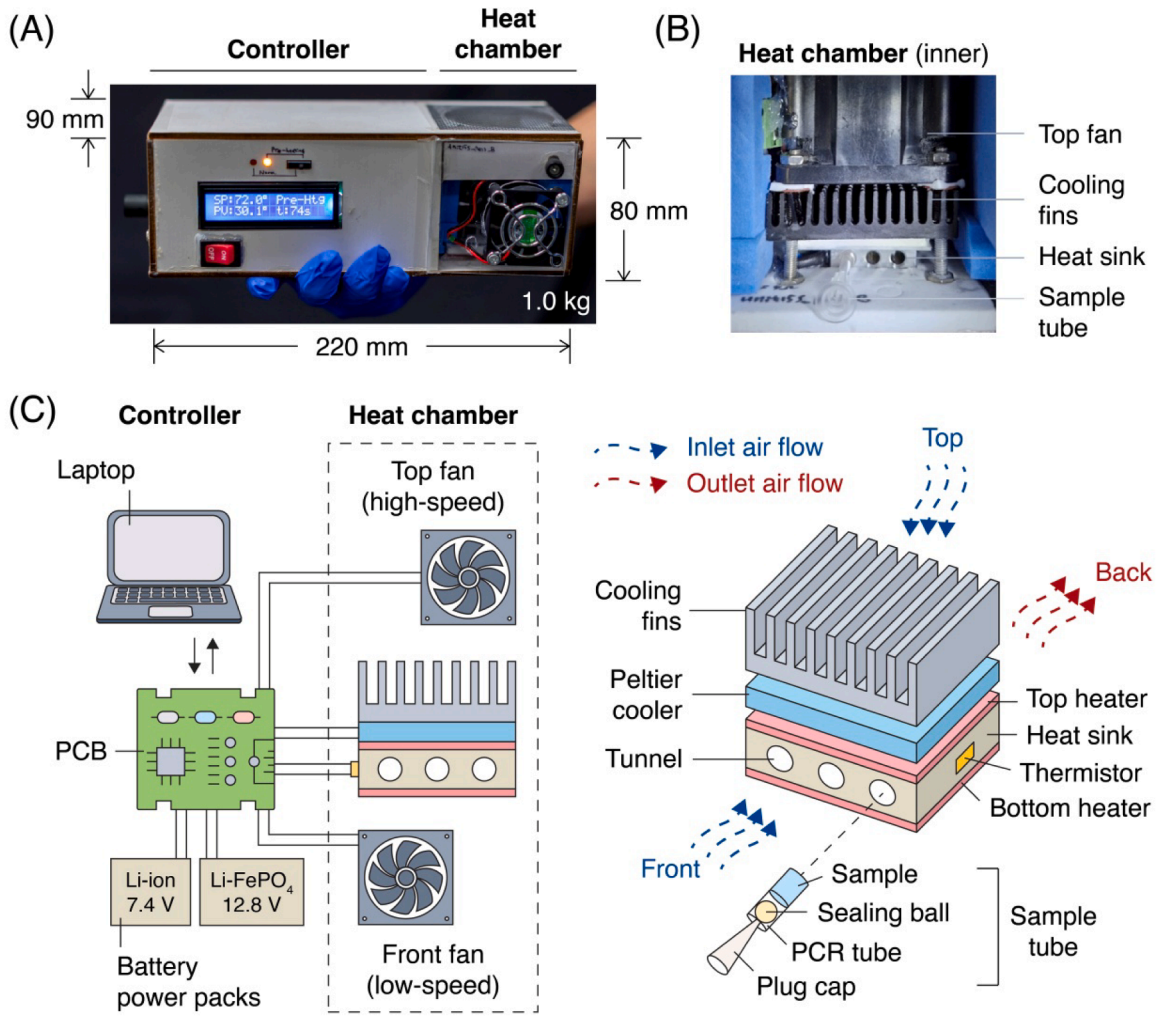


Fig. 1. Hand-held POCT-PCR thermocycler and heat chamber design. (A) External view of the handheld POCT-PCR thermocycler showing the control panel, including the LCD display, indicator LED, and input switches. (B) Internal structure of the heat chamber, comprising the top cooling fan, cooling fins, heat sink, and sample-tube positions. (C) Schematic layout of the thermocycler system, including the high-speed top cooling fan, aluminum fin array, Peltier cooler, dual ceramic heaters (top and bottom), aluminum heat sink with cylindrical sample tunnels, silicone PCR tube with sealing-ball plug cap, thermistor sensor, low-speed front cooling fan, PCB with Arduino-based PID control circuitry, dual battery packs, and optional PC interface for thermal-profile monitoring.

Daihan Scientific, Korea). One end was sealed with silicone sealant (3140 RTV, DuPont, USA), while the open end was closed with a polypropylene plug cap formed by reshaping a pipette tip into a spherical sealing ball ($\geq$ 2.24 mm in diameter, see section S3 in S1 File). This design improved thermal contact and minimized evaporation during cycling.

2.3. DNA sample preparation

Genomic DNA from eleven cyanobacterial species and corresponding primers (Tables S3 and S4) were used as templates. PCR reactions (20 μL) contained 2 μL DNA, 0.2 μL of each primer (10 pmol), 10 μL commercial premix (Dyne 2X PreMIX-HOT, Dyne Bio Inc., Korea), and nuclease-free water. For *Tolypothrix distorta* and *Limnothrix planctonica*, primer volumes were adjusted for optimal amplification. Amplification employed Taq DNA polymerase with standard denaturation–annealing–extension cycling conditions (Table 2).

All cyanobacterial strains were isolated samples provided by the Nakdonggang National Institute of Biological Resources (NNIBR, Sangju, Korea). Genomic DNA (gDNA) was individually extracted from each strain using a QIAamp® DNA Mini Kit (QIAGEN, Hilden, Germany) in accordance with the manufacturer's instructions. The cyanobacterial strains were morphologically identified by NNIBR prior to DNA extraction. Based on sequence information available in the NCBI GenBank database, rbcL universal and species-specific primers were designed to obtain rbcL sequences for each strain. Sequence trimming and alignment were performed using Sequencher version 4.7 (Gene Codes Corporation, MI, USA), and the resulting rbcL DNA sequences were analyzed using the NCBI BLAST program to confirm species identity. The amplified nucleotide sequences have been submitted to the NCBI GenBank database via the BankIt submission portal, and accession numbers are currently pending.

For the PCR-based selectivity assay, the template DNA used as the positive control consisted of a mixture of gDNA from ten species,

Table 2
Thermocyclic conditions for cyanobacteria PCR.

Phase	SP (°C)	Ramp time (s)	Duration (s)
Pre-heating[a]	72	30	180
Denaturation	94	20	30 (180)[b]
Annealing	55	20	30
Extension	72	10	30 (300)[b]
Total	-	50	90 (480)[b]

[a] Warming up to establish the identical state to the end of extension.
[b] Parentheses are the extended times to first and last cycles only.

including the target species. The template DNA used as the negative control consisted of a mixture of gDNA from nine non-target species, excluding the target species, and was used to evaluate assay specificity.

For electrophoretic analysis, PCR amplicons were separated using a standard agarose gel electrophoresis system in the laboratory. Commercial PCR premix reagents were maintained under the manufacturer-recommended storage conditions prior to amplification. During field validation experiments, reagents were transported in insulated containers with ice packs to preserve enzyme stability. Amplification reactions were prepared using sterile disposable pipette tips and pre-sealed reaction tubes, and amplification and post-PCR handling were physically separated to minimize potential cross-contamination. All relevant chemical and reagent materials were listed in Table S5.

2.4. Gel electrophoresis

PCR amplicons were analyzed by agarose gel electrophoresis. Gels (1 % w/v) were prepared in 1X TBE buffer with SYBR™ Safe DNA stain (Invitrogen, Thermo Fisher Scientific, USA). PCR products (5 μL) mixed with loading buffer were run alongside a 100 bp DNA ladder (Bioneer, Korea) at 100 V for 30 min. DNA fragments were visualized under blue light excitation using a Bento Lab transilluminator (Bento Bioworks Ltd., UK).

3. Results and discussion

3.1. POCT-PCR design rationale

As mentioned above, a central requirement for field-deployable PCR is the ability to combine rapid and reliable thermal cycling with portability and low power consumption [22]. Conventional benchtop thermocyclers, which typically rely on block heating of polypropylene tubes (50–100 μL), suffer from slow heat transfer, long ramping times, and frequent evaporation during high-temperature denaturation [23]. These limitations restrict their applicability in on-site diagnostics, particularly in resource-limited environments where bulky instrumentation, continuous power supply, and complex sample handling are impractical.

The POCT-PCR system was therefore designed as a lightweight, handheld thermocycler optimized for small-volume reactions, efficient heat transfer, and autonomous battery operation (Fig. 1A). The device integrates an aluminum heat sink with dual ceramic heaters for rapid heating, a Peltier-based cooling module with forced-air dissipation for efficient cooling, and a fast-response thermistor for real-time temperature monitoring (Fig. 1B and C). These components are regulated by an Arduino-based PID controller, which minimizes overshoot and undershoot to maintain stable thermal cycling. A dual rechargeable battery pack provides sufficient capacity for multiple runs without external power, ensuring true portability.

A second key design principle was to enhance sample integrity and evaporation control. Instead of conventional conical PCR tubes, we fabricated cylindrical silicone microtubes with reduced volume capacity (<30 μL) and optimized surface-to-volume ratios for efficient heat transfer [23,24]. The tubes are sealed with a plug-cap incorporating a spherical ball, which expands radially inside the chamber tunnel during heating. This design offers several advantages over conventional vertical PCR tubes, as discussed in section 3.5 [5,22].

These improvements not only minimized sample loss but also stabilized the reaction environment across multiple cycles. Importantly, the radial expansion of the elastomer tube and sealing ball is greater than that of the aluminum chamber (coefficients of thermal expansion: 150–250 × 10^{-6}/K vs. 24 × 10^{-6}/K), ensuring tighter sealing at high temperatures. As a result, evaporation was suppressed without additional mechanical compression, contributing to both the robustness and simplicity of the system.

Together, these features define POCT-PCR as a platform specifically engineered for rapid, low-cost, and field-deployable DNA amplification. In the following sections, we present its thermodynamic control, tube performance, and reproducibility in PCR amplification of cyanobacterial DNA, demonstrating the potential of this system for ecological surveillance and public health protection.

3.2. Temperature sensing

Accurate and stable thermal cycling is fundamental for PCR fidelity [21–23,35]. To achieve this, POCT-PCR employed a 10 kΩ NTC thermistor for temperature sensing, measured using a 10-bit analog-to-digital converter integrated into an Arduino microcontroller [35–39]. Resistance–temperature calibration using the Steinhart–Hart (S–H) equation (Eq. (1)) yielded an excellent fit to measured data, providing temperature accuracy within ±0.15°C across the PCR operating range (Fig. 2) [37]. Self-heating effects were negligible (<0.14°C), validating the reliability of the thermistor for precise PCR cycling (see section S1 in S1 File) [40–43].

$$\frac{1}{T} = A + B\ln R + C(\ln R)^3 \tag{1}$$

where T is absolute temperature, R the resistance, and A, B, C are the S–H coefficients.

3.3. PID control tuning

Thermal control was regulated by a PID controller (Fig. 3A) [16,44–48], which minimized the error between the setpoint (SP) and the process variable (PV), defined as $e(t) = \mathrm{SP} - \mathrm{PV} = r(t) - y(t)$, using the control function [47]:

$$c(t) = K_p e(t) + K_i \int_0^t e(\tau)\mathrm{d}\tau + K_d \frac{d}{dt} e(t) \tag{2}$$

where K_P, K_i, and K_d are the proportional, integral, and derivative gain parameters, respectively. Optimizing these parameters ensures that the controller output, $c(t)$, drives the thermocycler response, $y(t)$, to approach the SP quickly, accurately, and stably.

PID tuning was initiated using the heuristic Ziegler-Nichols method [44–46]. The proportional gain K_P in Eq. (2) was set to 1, with K_i and K_d at zero, and gradually increased. At $K_\mathrm{P} = 5$, an overdamped response was observed, failing to reach the SP with a high steady-state error, ΔT_s (Fig. 3B, black lines). Increasing K_P to 50 introduced underdamped

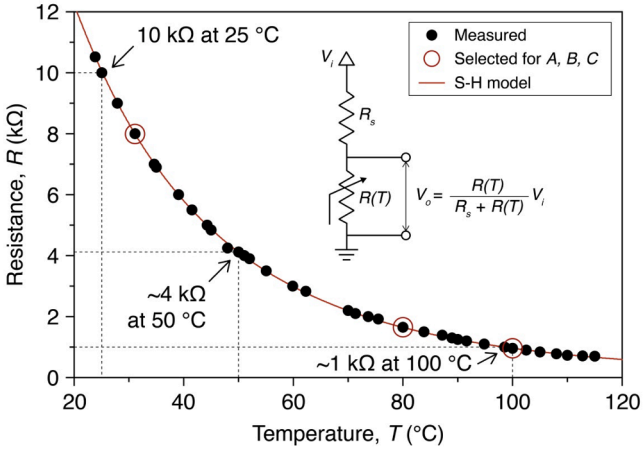
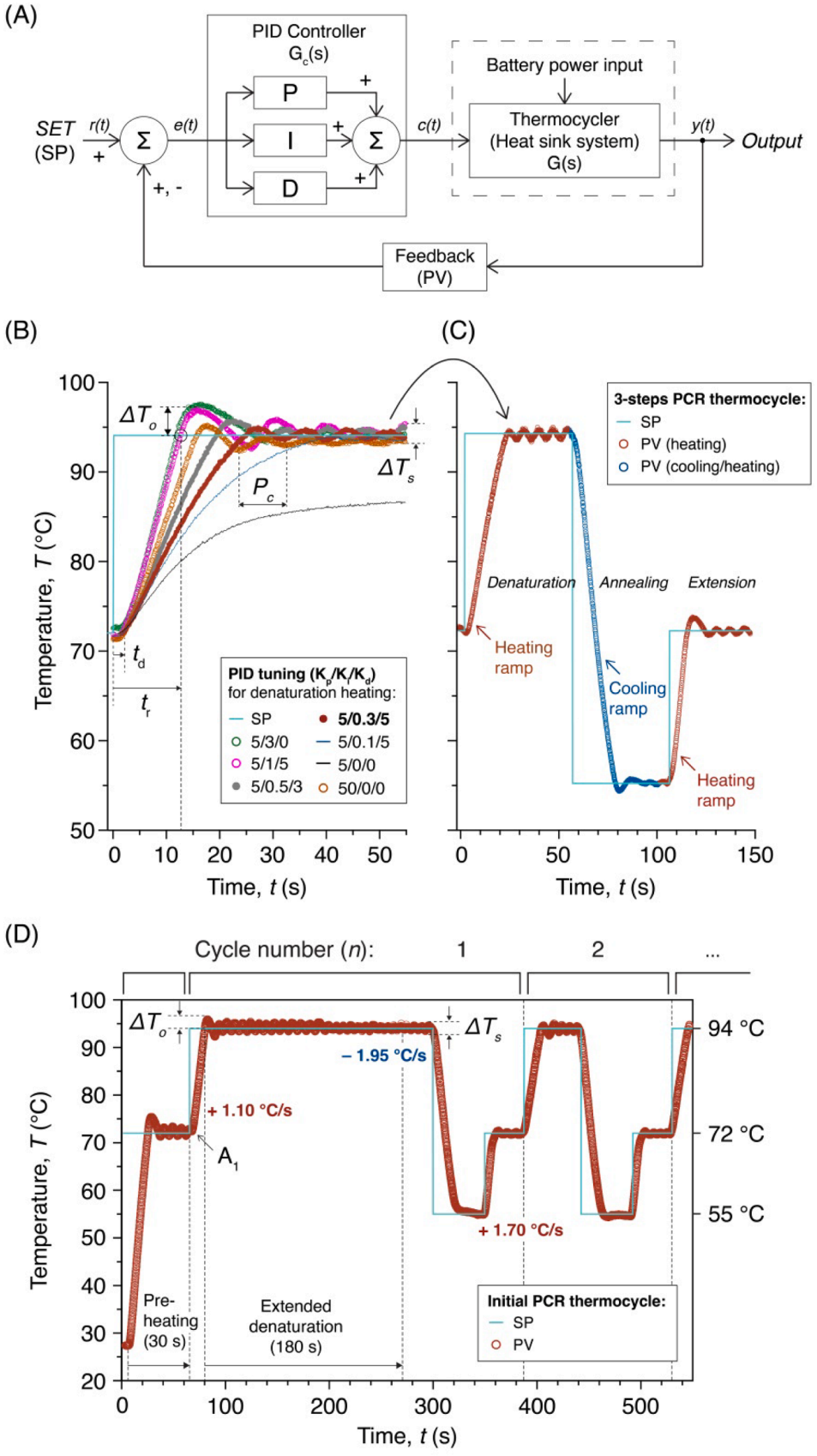


Fig. 2. Thermo-resistance calibration of the NTC thermistor using the Steinhart–Hart (S–H) equation. Measured resistance values (black dots) were fitted with the S–H model (red line). Three calibration points at 30, 80, and 100°C (red circles) were used to obtain the S–H coefficients. (Inset: voltage-divider circuit used to measure the thermistor output voltage, which was converted to resistance and subsequently to temperature via Eq. (1).).



(caption on next page)

Fig. 3. Optimization of PID control. (A) Block diagram of the closed-loop temperature control system consisting of the PID controller and the thermocycler heat-sink module. (B) Temperature responses under different PID parameter sets, showing overshoot (ΔT_o), steady-state error (ΔT_s), delay time (t_d), and rise time (t_r). (C) Optimized three-step PCR temperature profile demonstrating close agreement between the setpoint (SP, cyan) and the process variable (PV, red/blue) during denaturation, annealing, and extension. (D) Temperature trajectories for the initial PCR cycles. Cycle 1 exhibits slightly different behavior from cycle 2 due to transient thermal stabilization, whereas cycles $n > 2$ show highly reproducible and overlapping profiles.

oscillations with a period of $P_c \approx 10$ s, an initial overshoot of $\Delta T_o = 2.6°C$, and a steady-state error converging to $\Delta T_s \approx 0.1°C$ (Fig. 3B, orange circles). At $K_P = 200$, nearly undamped oscillations occurred (not shown).

Next, the integral gain K_i was tuned. Even a small $K_i = 0.1$, with $K_p = 5$, produced a critically damped response, approaching the SP asymptotically with a rise time of $t_r = 43$ s (time to reach SP after input activation) and a time constant of 17 s (time to reach 63 % of SP) (Fig. 3B, blue line). The temperature response was further investigated for fixed $K_p = 5$ with varying K_i: 0.5 (gray circles), 1 (magenta circles), and 3 (green circles). As K_i increased, the rise time decreased, but the overshoot ΔT_o increased.

Minimizing overshoot is critical for PCR thermocyclers, as Taq polymerase activity degrades above 95°C [5,23,49]. Through trial-and-error tuning, optimal parameters were achieved: $K_p = 5$, $K_i = 0.3$ and $K_d = 5$, yielding a minimal overshoot of $\Delta T_o < 0.7°C$ and a steady-state error of $|\Delta T_s| < 1.0°C$ (peak-to-peak) (Fig. 3B, red circles). These values deviated significantly from the Ziegler-Nichols recommendations ($K_P = 0.6K_c$, $K_i = 1.2K_c/P_c$, $K_d = 0.075K_cP_c$), calculated as (30, 6, 37.5) with critical gain $K_c = 50$ and period $P_c = 10$ s [44], indicating that the Ziegler-Nichols method is less effective for the POCT-PCR system due to its high K_i sensitivity [21,50].

To achieve a fast yet stable thermocycler, a slightly longer rise time ($t_r = 20$–25 s) was accepted to prioritize low ΔT_o and ΔT_s. Applying similar tuning to the annealing and extension phases, a three-phase PCR cycle was constructed, exhibiting a smooth temperature gradient (Fig. 3C). In hardware, the PID parameters were implemented via an Arduino microcontroller, which generates PWM voltages (manipulated variables) through MOSFETs to control heaters, a Peltier cooler, and two cooling fans [16,21,39].

These results confirm that the system achieves both accuracy and robustness in thermal cycling. While advanced system modeling using first-order and second-order transfer functions provided further insight into the control loop dynamics, these details are presented in the Supporting Information (Figs. S1 and S2 in S1 File).

3.4. Operational performance and reproducibility

The stability of the POCT-PCR system was assessed through repeated three-phase thermal cycling across 30 cycles. After an initial pre-heating stage, the device produced highly reproducible temperature profiles from the second cycle onward, with trajectories closely overlapping a standard reference curve (Fig. 3C). This reproducibility underscores the robustness of the PID control in maintaining stable denaturation, annealing, and extension phases under battery-powered operation. Unlike conventional PCR workflows, which require sample transport and laboratory infrastructure, the POCT-PCR system allows same-day molecular confirmation on-site, significantly reducing delays in HAB diagnostics.

Two distinct features were observed in the first cycle (Fig. 3D). First, the denaturation phase exhibited a larger overshoot ($\Delta T_o \approx 1.8°C$) compared with subsequent cycles ($\Delta T_o \approx 1.0°C$). This instability, caused by transient heat accumulation within the thermally insulated heat chamber, was effectively suppressed by extending the pre-heating time beyond 180 s, thereby reducing overshoot to $<1.0°C$ and ensuring steady-state deviations of $<0.34°C$. Second, the first annealing step showed a critically damped temperature response without undershoot, in contrast to the underdamped oscillations observed in later cycles. While non-standard, this effect proved advantageous for primer binding by enhancing specificity at the 55°C setpoint [5,23].

Across 30 cycles, the system achieved reproducible ramp rates of +1.10°C/s during denaturation, –1.95°C/s during annealing, and +1.70°C/s during extension. These rates allowed a complete 30-cycle protocol (including extended first denaturation and final extension steps, see Table 2) to be finished within 78 min, demonstrating performance comparable to or faster than other low-cost portable PCR systems [14,21,22]. Importantly, these results were achieved without requiring Peltier-based active heating, reducing overall power consumption and increasing suitability for field operation.

Collectively, these findings demonstrate that POCT-PCR delivers reproducible, stable thermal cycling with user-friendly operation. Even when initial instabilities occur, simple adjustments such as extended pre-heating, A_1, enable users to maintain fidelity, a critical advantage in resource-limited and field-based diagnostic settings.

3.5. Sample preservation and tube performance

Evaporation of aqueous samples is a critical limitation in conventional PCR, particularly when using 100 μL polypropylene tubes with large air–liquid interfaces [23,51–55]. In such formats, thermal cycling often leads to water loss, condensation, or leakage, which compromise amplification quality and reproducibility. Conventional strategies—such as overlaying mineral oil, applying grease or wax, or incorporating heated lids—can mitigate evaporation but add cost, complexity, and bulk to the system, making them impractical for lightweight field-deployable devices [52–56].

To address this, we developed cylindrical silicone mini-PCR tubes (capacity ~30 μL) sealed with plug-cap spherical balls after filling the sample using a syringe (Fig. 4A and B). This design minimizes headspace above the reaction mixture, maximizes radial thermal contact with the aluminum heat sink (Fig. 4C), and eliminates the need for oil overlays or lid heaters [52,57]. During thermal cycling, the elastomer tube and sealing ball undergo greater radial expansion than the surrounding aluminum chamber, producing a self-tightening seal that effectively suppresses evaporation and prevents leakage (Fig. 4D). Details in filling and sealing procedures are described in Supporting Information (sections S3 and S10 in S1 File).

The performance of these mini-tubes was directly compared with that of conventional PCR tubes. As shown in Fig. 5, properly sealed POCT-PCR tubes exhibited significantly reduced solution loss relative to 100 μL polypropylene tubes operated under identical cycling conditions. Importantly, when the sealing ball diameter exceeded a critical threshold ($\phi_b \geq 2.24$ mm), the tubes consistently preserved > 96.3 % of sample volume, surpassing the performance of conventional tubes of $<$ 95.7 % and resulting in a 15 % improvement (see section S4 in S1 File). These results demonstrate that the POCT-PCR tube design not only simplifies sample handling but also provides reliable sample integrity under repeated high-temperature cycles.

Together, these findings establish the POCT-PCR tube as a practical solution for small-volume field PCR, offering three distinct advantages: (i) ease of handling due to capillary retention of the sample within the tube [57], (ii) enhanced thermal transfer through complete surface contact with the heat sink [53–56], and (iii) precise control of air volume by adjusting the sealing ball position. By addressing the long-standing challenge of evaporation in miniaturized PCR systems, this design improves both reliability and portability of the POCT-PCR platform.

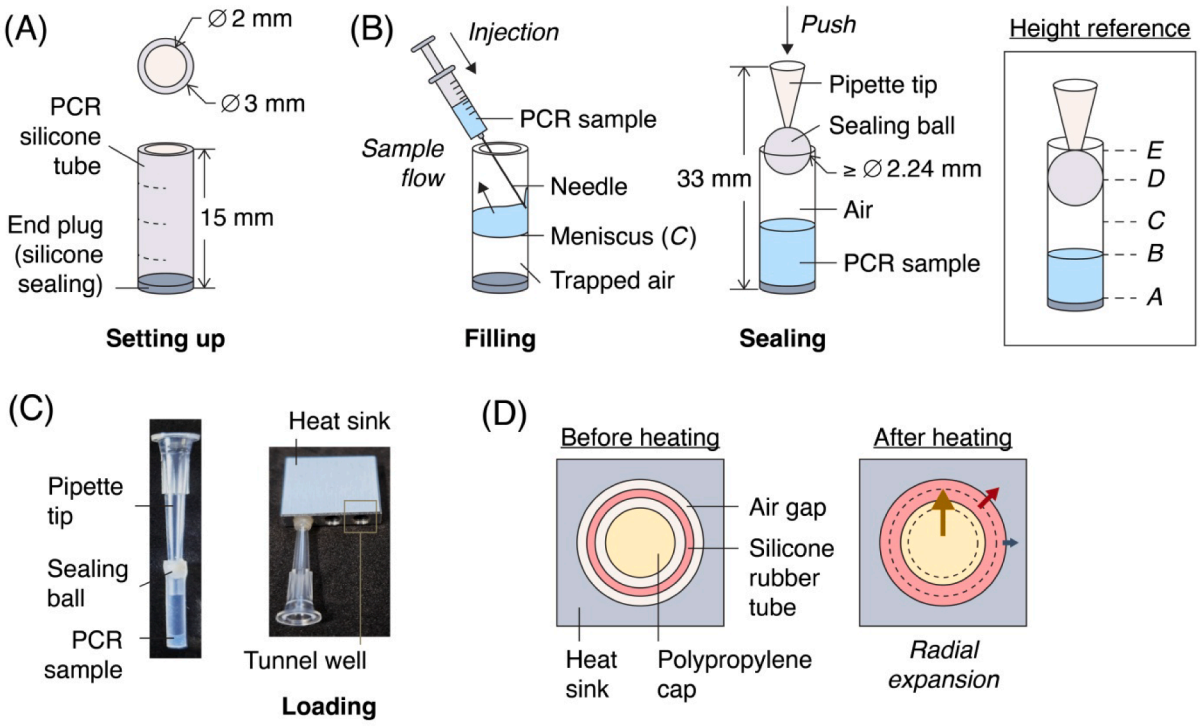


Fig. 4. Sample filling, sealing, and loading procedures. (A) Structure of the cylindrical silicone PCR tube and the polypropylene plug cap with a spherical sealing ball. (B) Sample filling and sealing procedure. The needle tip is positioned at the bottom end plug (reference height *A*) to prevent air trapping during injection. (C) Loading of the sealed PCR tube into the tunnel well of the heat sink. (D) Cross-sectional schematic illustrating thermal contact and radial expansion of the plug cap and silicone tube within the heat-sink tunnel, enabling tight sealing during heating.

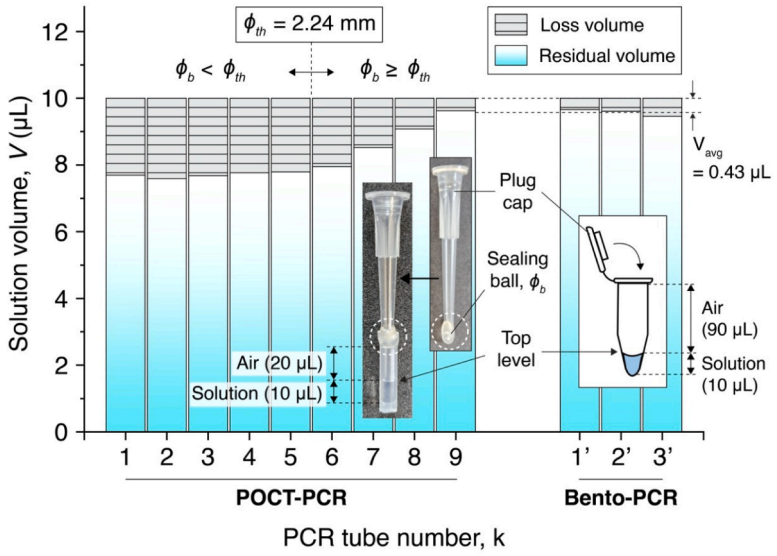


Fig. 5. Comparison of solution loss in POCT-PCR tubes and conventional 100 µL PCR tubes. Gray bars indicate loss volume, and cyan bars indicate residual volume after thermal cycling. Tube numbers (k) are arranged in order of increasing sealing-ball diameter. (Inset: designs of the POCT-PCR tube and plug-cap system and of conventional PCR tube).

3.6. Validation of cyanobacterial DNA amplification

To validate the biological performance of the POCT-PCR system and as a proof-of-concept demonstration for a real field deployable usage as shown in Fig. 6A, we tested its ability to amplify genomic DNA from multiple cyanobacterial species, including toxin-producing strains that are of particular concern in ecological monitoring. Because several of these taxa (e.g., *Microcystis, Anabaena*) are known producers of potent cyanotoxins, rapid molecular confirmation is directly linked to public-health risk assessment. As a representative case, amplification of *Leptolyngbya foveolara* (343 bp amplicon) consistently produced clear, well-defined bands (see Fig. 6B and section S12 in S1 File of the Supporting Information). Results obtained using POCT-PCR closely matched those from a commercial benchtop thermocycler, confirming equivalent amplification efficiency despite the handheld device's simplified and portable design.

Specificity of primer–template recognition was further assessed using both positive and negative control assays. In the positive control, a

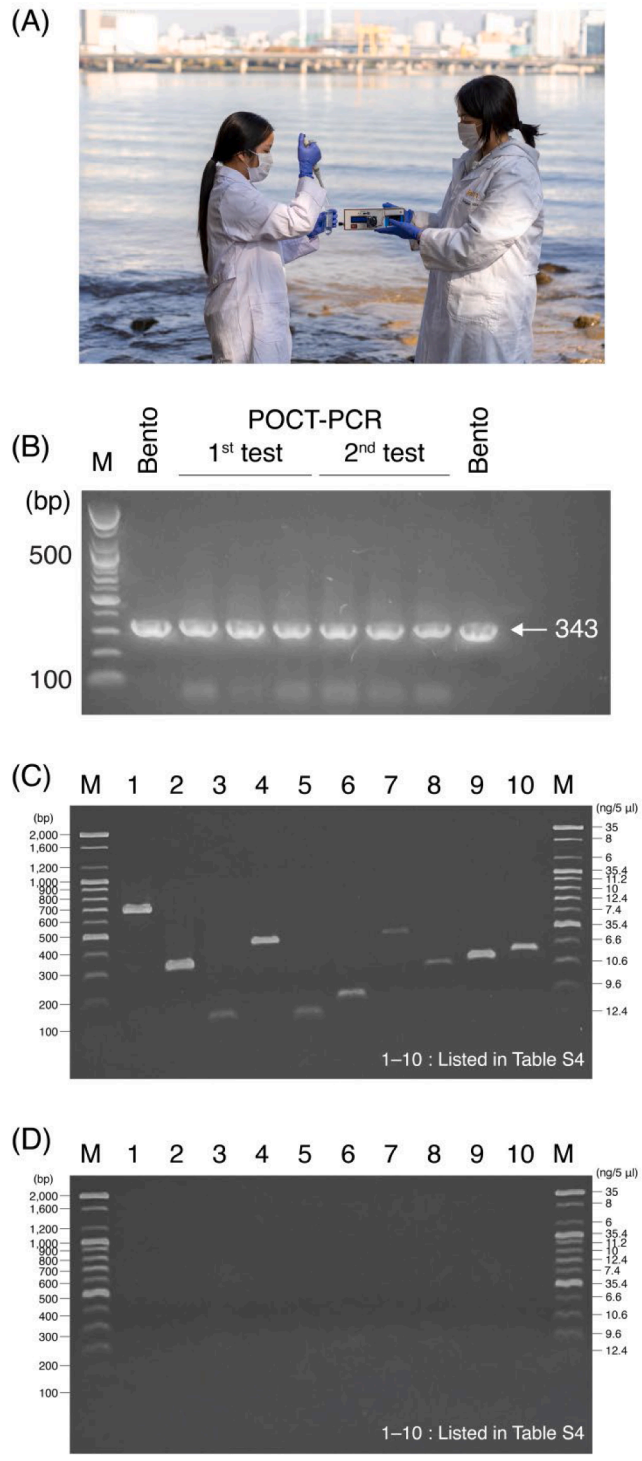


Fig. 6. Gel electrophoresis validation of PCR products. (A) Field demonstration of the POCT-PCR device at the Hangang River in Seoul. (B) Amplification of *Leptolyngbya foveolara* (343 bp). Results obtained using the commercial Bento PCR device [58] (lanes 1 and 8) are compared with those from the POCT-PCR device (lanes 2–7). (C) Positive controls showing amplification of ten cyanobacterial genes (100–700 bp). (D) Negative controls showing no detectable amplification, confirming primer specificity.

mixture of ten cyanobacterial templates was aliquoted into separate reactions, each with its species-specific primer pair. All ten targets were successfully amplified, generating distinct products ranging from 100 to 700 bp (Fig. 6C). In contrast, the negative control reactions, where the corresponding template DNA was deliberately omitted, produced no detectable products (Fig. 6D). These results confirm that POCT-PCR achieves high primer specificity and avoids cross-amplification, an essential requirement for field diagnostics where complex microbial backgrounds are expected.

Although band intensity varied slightly among targets, particularly for lanes 3, 5, 7, and 8 in the positive control, this effect is most likely attributable to primer design or template quality rather than limitations of the thermocycler itself. Importantly, these variations were reproducible across repeated runs, demonstrating that the device itself delivers stable amplification conditions.

Taken together, these results establish POCT-PCR as a robust and reliable platform for the on-site detection of multiple cyanobacterial species. This capability is particularly important for early-warning surveillance, as rapid confirmation of harmful cyanobacterial presence allows water managers to respond before bloom intensification or toxin accumulation occurs. By combining reproducibility with specificity, the system provides a strong foundation for early-warning programs aimed at safeguarding freshwater resources from harmful algal blooms. Beyond ecological applications, the demonstrated capability to detect diverse DNA targets highlights the broader potential of this system for field-deployable molecular diagnostics.

4. Conclusion

We developed the POCT-PCR system, a handheld, low-cost, and battery-powered thermocycler designed for rapid field detection of cyanobacteria. By integrating efficient thermal management, PID-controlled feedback, and custom-designed microtubes with robust sealing, POCT-PCR achieved fast ramp rates (+1.10°C/s heating, –1.95°C/s cooling), minimized evaporation, and maintained precise temperature stability within ±1.0°C. Validation assays confirmed reliable amplification of eleven cyanobacterial genes with reproducibility and specificity comparable to benchtop thermocyclers.

These findings demonstrate that POCT-PCR overcomes key limitations of conventional PCR systems of large sample volume, inefficient heat transfer, and high evaporation loss, while maintaining accuracy and portability. The system represents a practical, low-cost platform for ecological surveillance and public health applications, particularly for early and on-site detection of harmful algal blooms in freshwater reservoirs. Beyond environmental monitoring, the design principles presented here provide a foundation for expanding field-deployable molecular diagnostics in infectious disease detection, food safety, and environmental early-warning systems in resource-limited settings. In addition, the POCT-PCR platform could be rapidly deployed in urgent situations, such as infectious disease outbreaks or harmful bloom events, where on-site molecular confirmation is critical. Future improvements, including smartphone-based operation and wireless data acquisition, may further enhance accessibility and enable real-time data sharing in distributed field environments.

CRediT authorship contribution statement

Ignasia Handipta Mahardika: Validation, Investigation, Formal analysis. **Eunjin Huh:** Methodology, Investigation, Data curation. **Yoseph Seo:** Methodology, Investigation, Data curation. **Sarath Kin:** Visualization, Validation, Methodology, Data curation. **Semin Chun:** Methodology, Investigation. **Sang Ho Lee:** Visualization, Validation, Software. **Sohyun Nam:** Investigation, Data curation. **Soo Ryeon Ryu:** Methodology, Formal analysis. **So Jung Kim:** Investigation. **Shinwoo Kang:** Methodology, Investigation. **Wonseok Chung:** Investigation. **Junhong Min:** Resources, Methodology, Formal analysis, Data curation. **Taek Lee:** Writing – review & editing, Resources, Methodology, Funding acquisition, Formal analysis. **Oh-Sun Kwon:** Writing – original draft, Visualization, Validation, Methodology, Investigation, Data curation. **Kwanwoo Shin:** Writing – review & editing, Supervision, Project administration, Methodology, Funding acquisition, Conceptualization.

Declaration of competing interest

The authors declare that they have no known competing financial interests or personal relationships that could have appeared to influence the work reported in this paper.

Acknowledgments

This research was supported by Basic Science Research Programs (2020R1I1A1A01073311, 2018R1A6A1A03024940), and the Advanced Bio-Interface Core Research Facility, Sogang University (2020R1A6C101A192) through the National Research Foundation of Korea funded by the Ministry of Education, Science and Technology; and a grant program (RE202002043) funded by Korea Environmental Industry & Technology Institute (KEITI).

Supplementary materials

Supplementary material associated with this article can be found, in the online version, at doi:10.1016/j.talo.2026.100644.

Appendix A. Abbreviations

The following abbreviations are used in this manuscript:
DNA – Deoxyribonucleic acid
gDNA – Genomic DNA
HAB – Harmful algal bloom
NTC – Negative temperature coefficient
PCR – Polymerase chain reaction
PDMS – Polydimethylsiloxane
PID – Proportional–integral–derivative
POCT – Point-of-care testing
POCT-PCR – Point-of-care testing polymerase chain reaction

Appendix B. Supplementary data

Supporting Information associated with this article including supplementary data can be found online.
S1 File. Supporting document (PDF)
S2 File. Movie clip for POCT-PCR operational demonstration (MP4)
S3 File. Image file of circuit diagram (JPG)
S4 File. Gerber files for PCB manufacture (ZIP)
S5 File. Fritzing file for circuit diagram and Arduino coding (FZZ)
S6 File. AutoCAD file for case design (DWG)

Data availability

Data will be made available on request.

References

[1] K. Mullis, F. Faloona, S. Scharf, R. Saiki, G. Horn, H. Erlich, Specific enzymatic amplification of DNA In vitro: the polymerase chain reaction, Cold Spring Harb. Symp. Quant. Biol. 51 (1986) 263–273, https://doi.org/10.1101/SQB.1986.051.01.032.
[2] J. Singh, N. Birbian, S. Sinha, A. Goswami, A critical review on PCR, its types and applications, Int. J. Adv. Res. Biol. Sci. 1 (2014) 65–80. https://ijarbs.com/cissueoct.html.
[3] H. Zhu, H. Zhang, Y. Xu, S. Laššáková, M. Korabečná, P. Neužil, PCR past, present and future, Biotechniques 69 (2020) 317–325, https://doi.org/10.2144/btn-2020-0057.
[4] K. Vajpayee, V. Paida, R.K. Shukla, Nanoparticle-assisted PCR: fundamentals, mechanisms, and forensic implications, Int. J. Legal Med. 139 (2025) 945–964, https://doi.org/10.1007/s00414-024-03402-0.
[5] M. McPherson, S. Møller, PCR, 2nd ed., Taylor & Francis, 2006, pp. 9–85, https://doi.org/10.4324/9780203002674.
[6] M. Kubista, J.M. Andrade, M. Bengtsson, A. Forootan, J. Jonák, K. Lind, R. Sindelka, R. Sjöback, B. Sjögreen, L. Strömbom, A. Ståhlberg, N. Zoric, The real-time polymerase chain reaction, Mol. Aspects Med. 27 (2006) 95–125, https://doi.org/10.1016/j.mam.2005.12.007.
[7] M. Sawano, K. Takeshita, H. Ohno, H. Oka, RT-PCR diagnosis of COVID-19 from exhaled breath condensate: a clinical study, J. Breath Res. 15 (2021) 037103, https://doi.org/10.1088/1752-7163/ac0414.
[8] P. Liu, T.S. Seo, N. Beyor, K.-J. Shin, J.R. Scherer, R.A. Mathies, Integrated portable Polymerase chain reaction-capillary electrophoresis microsystem for rapid forensic short tandem repeat typing, Anal. Chem. 79 (2007) 1881–1889, https://doi.org/10.1021/ac061961k.
[9] K.M. Manali, R. Arunraj, G.S. Ramakrishnan, M. Ramya, Development of sensitive and specific multiplex PCR method for the detection of microcystin producing cyanobacteria in spirulina food supplements, Food Sci. Biotechnol. 28 (2019) 609–614, https://doi.org/10.1007/s10068-018-0476-0.
[10] J. Yuan, H.-J. Kim, C.T. Filstrup, B. Guo, P. Imerman, S. Ensley, K.-J. Yoon, Utility of a PCR-based method for rapid and specific detection of toxigenic microcystis spp. in farm ponds, J. Vet. Diagn. Invest. 32 (2020) 369–381, https://doi.org/10.1177/1040638720916156.
[11] Y. Zhou, F. Pei, M. Ji, L. Wang, H. Zhao, H. Li, W. Yang, Q. Wang, Q. Zhao, Y. Wang, Sensitivity evaluation of 2019 novel coronavirus (SARS-CoV-2) RT-PCR detection kits and strategy to reduce false negative, PLoS ONE 15 (2020) e0241469, https://doi.org/10.1371/journal.pone.0241469.
[12] P. Neuzil, Ultra fast miniaturized real-time PCR: 40 cycles in less than six minutes, Nucleic Acids Res. 34 (2006), https://doi.org/10.1093/nar/gkl416 e77–e77.
[13] J. Jie, S. Hu, W. Liu, Q. Wei, Y. Huang, X. Yuan, L. Ren, M. Tan, Y. Yu, Portable and battery-powered PCR device for DNA amplification and fluorescence detection, Sensors 20 (2020) 2627, https://doi.org/10.3390/s20092627.
[14] J. An, Y. Jiang, B. Shi, D. Wu, W. Wu, Low-cost battery-powered and user-friendly real-time quantitative PCR system for the detection of multigene, Micromachines 11 (2020) 435, https://doi.org/10.3390/mi11040435.
[15] L. He, B. Sang, W. Wu, Battery-powered portable rotary real-time fluorescent qPCR with low energy consumption, low cost, and high throughput, Biosensors 10 (2020) 49, https://doi.org/10.3390/bios10050049.
[16] G.T. İnce, M. Yüksekkaya, O.E. Haberal, Polymerase chain reaction microchip and PID controller based thermal cycler design, Int. J. Multidiscip. Res. 6 (2024), https://doi.org/10.36948/ijfmr.2024.v06i01.13763.
[17] P.-A. Auroux, P.J.R. Day, A. Manz, Sample-shunting based PCR microfluidic device, TechConnect Briefs 1 (2004) 67–69. https://briefs.techconnect.org/papers/sample-shunting-based-pcr-microfluidic-device/. accessed August 4, 2025.
[18] I. Schneegaß, R. Bräutigam, J.M. Köhler, Miniaturized flow-through PCR with different template types in a silicon chip thermocycler, Lab Chip 1 (2001) 42–49, https://doi.org/10.1039/B103846J.
[19] D. Wu, W. Wu, Battery powered portable thermal cycler for continuous-flow polymerase chain reaction diagnosis by single thermostatic thermoelectric cooler and open-loop controller, Sensors 19 (2019) 1609, https://doi.org/10.3390/s19071609.
[20] J.S. Farrar, C.T. Wittwer, Extreme PCR: efficient and specific DNA amplification in 15–60 seconds, Clin. Chem. 61 (2015) 145–153, https://doi.org/10.1373/clinchem.2014.228304.
[21] T. Kadja, C. Liu, Y. Sun, V.P. Chodavarapu, Low-cost, real-time polymerase chain reaction system for point-of-care medical diagnosis, Sensors 22 (2022) 2320, https://doi.org/10.3390/s22062320.
[22] K. Luo, W. Cheng, Y. Chen, Q. Zhang, C. Liang, J. Li, W. Wang, A portable low-cost polymerase chain reaction device, HardwareX 21 (2025) e00635, https://doi.org/10.1016/j.ohx.2025.e00635.
[23] Y.Ho Kim, I. Yang, Y.-S. Bae, S.-R. Park, Performance evaluation of thermal cyclers for PCR in a rapid cycling condition, BioTechniques 44 (2008) 495–505, https://doi.org/10.2144/000112705.
[24] R.P. Oda, M.A. Strausbauch, A.F.R. Huhmer, N. Borson, S.R. Jurrens, J. Craighead, P.J. Wettstein, B. Eckloff, B. Kline, J.P. Landers, Infrared-mediated thermocycling for ultrafast polymerase chain reaction amplification of DNA, Anal. Chem. 70 (1998) 4361–4368, https://doi.org/10.1021/ac980452i.
[25] C.D. Ahrberg, J.W. Choi, J.M. Lee, K.G. Lee, S.J. Lee, A. Manz, B.G. Chung, Plasmonic heating-based portable digital PCR system, Lab Chip 20 (2020) 3560–3568, https://doi.org/10.1039/D0LC00788A.
[26] C.T. Wittwer, G.C. Fillmore, D.J. Garling, Minimizing the time required for DNA amplification by efficient heat transfer to small samples, Anal. Biochem. 186 (1990) 328–331, https://doi.org/10.1016/0003-2697(90)90090-V.
[27] D. Braun, N.L. Goddard, A. Libchaber, Exponential DNA replication by laminar convection, Phys. Rev. Lett. 91 (2003) 158103, https://doi.org/10.1103/PhysRevLett.91.158103.
[28] X. Yang, C. Guo, Q. Zhang, Y. Chen, Y. Liu, X. Zhang, A portable thermostatic molecular diagnosis device based on high-efficiency photothermal conversion material for rapid field detection of SARS-CoV-2, Talanta 258 (2023) 124422, https://doi.org/10.1016/j.talanta.2023.124422.
[29] M.B. Kulkarni, S. Goel, Mini-Thermal platform integrated with microfluidic device with on-site detection for real-time DNA amplification, BioTechniques 74 (2023) 158–171, https://doi.org/10.2144/btn-2022-0091.
[30] N.J. Smucker, J.J. Beaulieu, C.T. Nietch, J.L. Young, Increasingly severe cyanobacterial blooms and deep water hypoxia coincide with warming water temperatures in reservoirs, Global Change Biology 27 (2021) 2507–2519, https://doi.org/10.1111/gcb.15618.
[31] R. Mohan, T. Sathish, K.B. Padmakumar, Occurrence of potentially toxic cyanobacteria microcystis aeruginosa in aquatic ecosystems of central Kerala (south India), Ann. Limnol. - Int. J. Lim. 56 (2020) 18, https://doi.org/10.1051/limn/2020015.
[32] N.Y. Park, H.S. Choi, S.U. Kang, A.S. Lim, The harmful cyanobacterium *microcystis aeruginosa* differently affects the growth rate and photosynthetic efficiency of

several species of marine phytoplankton, Environ. Microbiol. Rep. 17 (2025) e70091, https://doi.org/10.1111/1758-2229.70091.
[33] Y. Kawashima, T. Akasaki, Y. Matsumoto, S. Shimada, Development of a rapid and accurate PCR-based detection method for commercially valuable green algal species, Fish Sci. 80 (2014) 859–867, https://doi.org/10.1007/s12562-014-0760-8.
[34] G. Yuan, S. Gao, J.J. Czajka, Z. Dai, K.R. Pomraning, R.D. Duong, B.A. Hofstad, S. Deng, Simple and effective squash-PCR for rapid genotyping of industrial microalgae, Life 14 (2024) 115, https://doi.org/10.3390/life14010115.
[35] C.S. Laorden, Simulation and experimental validation of temperature inside PCR reaction chambers of a fully-integrated analytical system, Universitat Oberta de Catalunya (UOC), 2024. https://hdl.handle.net/10609/151579 (accessed August 4, 2025).
[36] P.R.N. Childs, J.R. Greenwood, C.A. Long, Review of temperature measurement, Rev. Sci. Instrum. 71 (2000) 2959–2978, https://doi.org/10.1063/1.1305516.
[37] M. Petkovšek, M. Nemec, P. Zajec, Algorithm execution time and accuracy of NTC thermistor-based temperature measurements in time-critical applications, Mathematics 9 (2021) 2266, https://doi.org/10.3390/math9182266.
[38] M. Grossi, M. Omaña, Accuracy of NTC thermistor measurements using the sensor to microcontroller direct interface, Eng. Proc. 82 (2024) 12, https://doi.org/10.3390/ecsa-11-20527.
[39] D.K. Fisher, P.J. Gould, Open-source hardware is a low-cost alternative for scientific instrumentation and research, Mod. Instrum. 1 (2012) 8–20, https://doi.org/10.4236/mi.2012.12002.
[40] M. Sapoff, R.M. Oppenheim, Theory and application of self-heated thermistors, in: Proceedings of the IEEE, 1963, pp. 1292–1305, https://doi.org/10.1109/PROC.1963.2560.
[41] Z. Liu, P. Huo, C. Shi, Y. Yan, F. Kong, S. Cao, A. Chang, J. Wang, J. Yao, Design of temperature measurement system guided by thermal dissipation coefficient of NTC thermistor, Sens. Actuators A-Phys. 377 (2024) 115772, https://doi.org/10.1016/j.sna.2024.115772.
[42] H. Ebrahimi-Darkhaneh, Measurement error caused by self-heating in NTC and PTC thermistors, Analog Design J. (2019). https://www.ti.com/lit/pdf/slyt774.
[43] NTC thermistors – general technical information, TDK/EPCOS AG, 2018. https://www.tdk-electronics.tdk.com/download/531116/19643b7ea798d7c4670141a88cd993f9/pdf-general-technical-information.pdf (accessed August 1, 2025).
[44] A.K. Sukede, J. Arora, Auto tuning of PID controller, in: Proc. Int. Conf. Ind. Instrum. Control (ICIC), IEEE Xplore, Pune, India, 2015, pp. 1459–1462, https://doi.org/10.1109/IIC.2015.7150979.
[45] P.V. Gopi Krishna Rao, M.V. Subramanyam, K. Satyaprasad, Study on PID controller design and performance based on tuning techniques, in: Proc. Int. Conf. Control, Instrumentation, Communication and Computational Technologies (ICCICCT), IEEE Xplore, Kanyakumari, India, 2014, pp. 1411–1417, https://doi.org/10.1109/ICCICCT.2014.6993183.
[46] S. Li, Q. Jiang, Study on pid parameters tuning method based on Matlab/Simulink, in: 2011 IEEE 3rd International Conference on Communication Software and Networks, 2011, pp. 408–411, https://doi.org/10.1109/ICCSN.2011.6014596.
[47] K.J. Åström, T. Hägglund, PID Controllers: Theory, Design, and Tuning, Second Edition, Instrument Society of America, Research Triangle Park, NC, 1995. https://www.isa.org/products/pid-controllers-theory-design-and-tuning-secon-1. accessed August 5, 2025.
[48] P. Woolf, Chapter 9: PROPORTIONAL-INTEGRAL-DERIVATIVE (PID) CONTROL, in: P. Woolf (Ed.), Chemical Process Dynamics and Controls, LibreTexts, 2007, pp. 710–732, in: https://eng.libretexts.org/Bookshelves/Industrial_and_Systems_Engineering/Chemical_Process_Dynamics_and_Controls_(Woolf)/09%3A_Proportional-Integral-Derivative_(PID)_Control/9.06%3A_PID_Downsides_and_Solutions. accessed August 5, 2025.
[49] E. van Pelt-Verkuil, R. te Witt, Part 1: technical backgrounds and quality aspects, in: E. van Pelt-Verkuil, W.B. van Leeuwen, R. te Witt (Eds.), Molecular Diagnostics, Springer Nature Singapore Pte Ltd., Singapore, 2019, pp. 131–143, https://doi.org/10.1007/978-981-13-1604-3_4.
[50] Z.Q. Niu, W.Y. Chen, S.Y. Shao, X.Y. Jia, W.P. Zhang, DNA amplification on a PDMS–glass hybrid microchip, J. Micromech. Microeng. 16 (2006) 425, https://doi.org/10.1088/0960-1317/16/2/029.
[51] V. Sailaja, R. Datla, K. Raju, M.L. Prasad, Design and development of embedded system based PCR thermal cycler, IOSR J. Electr. Electron. Eng. 14 (2019) 45–53, https://doi.org/10.9790/1676-1403034553.
[52] D.R. Sparkman, Paraffin wax as a vapor barrier for the PCR, Genome Res. 2 (1992) 180–181, https://doi.org/10.1101/gr.2.2.180.
[53] M. Span, M. Verblakt, T. Hendrikx, Comparison of temperature dynamics of various thermal cycler calibration methods, in: 19th International Congress of Metrology, 2019 19003, https://doi.org/10.1051/metrology/201919003.
[54] J.G. Atwood, A.C. Mossa, L.M. Goven, F. Williams, T.M. Woudenberg, M. Margoulies, R.P. Ragusa, R. Leath, C. Miles, Thermal cycler for automatic performance of the polymerase chain reaction with close temperature control, US5475610A, 1995. https://patents.google.com/patent/US5475610A/tr (accessed August 5, 2025).
[55] A. Tretiakov, H.-P. Saluz, Rapid heat block thermocycler, US6556940B1, 2003. https://patents.google.com/patent/US6556940B1/en?oq=US+Patent+6%2c556%2c940+B1 (accessed August 5, 2025).
[56] M.A. Hares, Thermal optimization for enabling PCR compatibility in acoustic MIicroplate systems. Dessertation, Purdue University, 2025, https://doi.org/10.25394/PGS.28828049.v1.
[57] Bio Rad PTC 100 Operations Manual, MJ Research Incoporated in Bio-Rad Inc., MA, USA, 1997. https://archive.org/details/manual_Bio-Rad_PTC-100_Operations_Manual. accessed August 5, 2025.
[58] K. Enya, S. Sasaki, T. Kunieda, A polymerase chain reaction experiment using *Escherichia coli* and Mars sand simulant for detection and analysis of extraterrestrial life, Life Sci. Space Res. 42 (2024) 84–90, https://doi.org/10.1016/j.lssr.2024.05.003, accessed August 5, 2025.